A particle-based elastic wave simulation method in 3D arbitrary anisotropic media using GPU

Pinghao Wang[1], Xiaofeng Jia[1], 1.School of Earth and Space Sciences, University of Science and Technology of China, Anhui, China*

Summary

The particle based dynamic lattice method (DLM) can simulate the elastic wave propagation in 3D arbitrary anisotropic media with a body-centered cube model. The connection between the microscopic interactions in the anisotropic lattice model and the macroscopic parameters such as the elasticity tensor are presented. Therefore, basing on the dynamic lattice method, we can use the body-centered cube lattice model to represent anisotropic media and simulate various dynamic behavior such as wave propagation. Additionally, we use GPU to accelerate our calculation, and the numerical test shows the usefulness of our method.

Introduction

Forward modeling of the behavior for the geological materials is always a fundamental issue in seismology. Although the equations in continuum theory reveal the mechanics of these material, analytical solutions to these equations only work for simple media. This leads to the development of various numerical methods. In terms of elastic wave simulation, numerical techniques such as the finite element methods (FEMs; e.g., Lysmer and Drake, 1972), the finite difference methods (FDMs; e.g., Madariaga 1976; Kelly et al. 1976; Virieux 1984,1986; Saenger et al. 2000) are widely used to give approximate solutions to wave equation. These numerical methods are still undergoing a lot of process. However, these wave equation based methods only apply to wave modeling; simulating other dynamic behaviors such as fracturing and deformation calls for another category of particle based methods. Based on the solid-state physics model of crystalline materials (Hoover et al. 1974) the distinct element method (Cundall & Strack 1979) represents one of the earliest particle based methods. Basing these studies, O'Brien & Bean (2004a,2004b) bring up a particle based elastic lattice method for 3D elastic wave simulation with topography and use this method to study volcano earthquake. O'brien et al. (2009) give detailed discussion on the dispersion properties and computational efficiency of this elastic lattice method. Xia et al. (2017) shows the implementation of the several lattice spring models in wave simulation.

The above methods all deal with elastic wave simulation in isotropic media. As for anisotropic case, difficulty lies in building the right anisotropic lattice model. To overcome this challenge, Hu and Jia (2016) bring up the dynamic lattice method where a 2-dimensional anisotropic lattice model is designed for elastic wave simulation in TTI media. Latter Hu and Jia (2018) establish the theory of high-order DLM to suppress spatial dispersion during wave simulation. The major purpose of this article is to expand the application of the DLM to elastic wave modeling in 3D complex anisotropic media. In this article, a 3D body-centered lattice model used for elastic wave simulation in 3D anisotropic media is introduced. We show the particle interaction patterns in this particular lattice model and demonstrate the general relation between the lattice model and the anisotropic media. We also use GPU to accelerate the calculation of the wave propagation in 3D model. In the numerical example, we carry out elastic wave simulations in 3D arbitrary anisotropic media.

3D arbitrary anisotropic lattice model

Building the particle lattice is the most crucial part of the dynamic lattice method. To simulate 3D arbitrary anisotropic media, we employ a body-centered lattice model shown in figure 1. In the basic lattice unit, the central particle is connected with its 18 neighboring particles through lattice bonds. As figure 2 shows, these bonds work like linear springs while the angles between these bonds are regarded as angular springs. The coefficients k_{ij} is used to describe the stiffness of the linear spring between particles i and j while the coefficient b_{ijk} represents the stiffness of the angular spring connecting particles i, j and k with the particle i as the pivot. The pattern and the stiffness coefficients of these bonds along with the mass of the particles define the elastic properties of the lattice model.

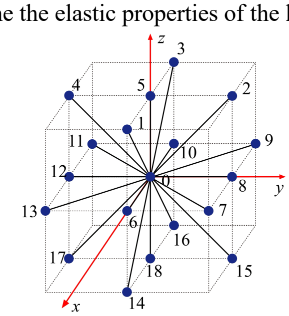

Figure 1: One particle lattice unit for the 3D lattice model. The central particle is connected with its 18 neighboring particles through lattice bonds.

In the case of anisotropy, the angular springs exist in the *xy-,xz-,yz-* planes (e.g., figures 3a) as well as four hexagonal planes(e.g., figures 3b). The balanced angles between the angular springs of *xy-,xz-,yz-* planes are $\frac{\pi}{2}$ while in the four hexagonal planes the balanced angles between the angular springs are $\frac{\pi}{3}$. The elastic energy in the lattice unit is given by

$$E=\frac{1}{2}\sum_{i}k_{0i}(|\mathbf{r}_{0i}|-|\mathbf{R}_{0i}|)^2+\frac{1}{2}\sum_{j,k}b_{j0k}(\cos\theta_{j0k}-\cos\theta^{0}{}_{j0k})^2 \tag{1}$$

where $\boldsymbol{r}_{0i}$ and $\boldsymbol{R}_{0i}$ respectively represent the vectors of bond that connects particle *0* and *i* in the distorted and undistorted lattices. Similarly, θ_{j0k} and θ^0_{j0k} are the angles between bonds *0-j* and *0-k* in the distorted and undistorted lattices respectively. The first sum of the equation is taken over half of the linear springs in the lattice unit to avoid double counting of the linear spring. The second term sums over all angular springs that use particle *0* as their pivots and the particle *j, k* are adjacent particles.

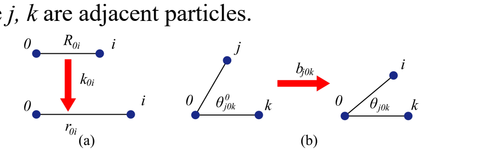

Figure 2. Stretching and bending of the bonds. (a) linear springs before and after distortion (b) angular springs before and after distortion. Red arrows denote the distortion of the particles.

Assuming that the relative displacement between the pairwise particles is much smaller than the length of bond that connects them, i.e. $|\boldsymbol{u}_i-\boldsymbol{u}_0|\ll|\boldsymbol{R}_{0i}|$ where $\boldsymbol{u}_i$ and $\boldsymbol{u}_0$ respectively represent the displacements of particles *i* and *0*, we can rewrite equation 1 as

$$E=\frac{1}{2}\sum_{i}k_{0i}\left(\frac{(\mathbf{u}_i-\mathbf{u}_0)\cdot\mathbf{R}_{0i}}{|\mathbf{R}_{0i}|}\right)^2+\frac{1}{2}\sum_{j,k}b_{j0k}\left[(\mathbf{u}_j-\mathbf{u}_0)\cdot\mathbf{s}_{kj}+(\mathbf{u}_k-\mathbf{u}_0)\cdot\mathbf{s}_{jk}\right]^2 \tag{2}$$

where $\mathbf{s}_{kj}=\dfrac{\mathbf{R}_{0k}\times\mathbf{R}_{0j}\times\mathbf{R}_{0j}}{|\mathbf{R}_{0k}||\mathbf{R}_{0j}|^3}$

In our body-centered lattice model, the total elastic energy counts the three *xy-, xz-, yz-* planes and the four hexagonal planes. Differentiating the elastic energy in equation 2 with respect to the particle displacements yields the interaction forces on the corresponding particles. Therefore, the interaction force on the central particle *0* is given by

$$\mathbf{F}_0=\frac{\partial E}{\partial\mathbf{u}_0}=\sum_{i}-k_{0i}\left(\frac{(\mathbf{u}_i-\mathbf{u}_0)\cdot\mathbf{R}_{0i}}{|\mathbf{R}_{0i}|^2}\right)\cdot\mathbf{R}_{0i}-\sum_{j,k}b_{j0k}\left[(\mathbf{u}_j-\mathbf{u}_0)\cdot\mathbf{s}_{kj}+(\mathbf{u}_k-\mathbf{u}_0)\cdot\mathbf{s}_{jk}\right](\mathbf{s}_{kj}+\mathbf{s}_{jk}) \tag{3}$$

And for non-central particle *i*, the interaction force takes the form as

$$\mathbf{F}_i=\frac{\partial E}{\partial\mathbf{u}_i}=k_{0i}\left(\frac{(\mathbf{u}_i-\mathbf{u}_0)\cdot\mathbf{R}_{0i}}{|\mathbf{R}_{0i}|^2}\right)\cdot\mathbf{R}_{0i}+\sum_{k}b_{i0k}\left[(\mathbf{u}_i-\mathbf{u}_0)\cdot\mathbf{s}_{ki}+(\mathbf{u}_k-\mathbf{u}_0)\cdot\mathbf{s}_{ik}\right]\cdot\mathbf{s}_{ki} \tag{4}$$

The summation for the second term in the right hand side of equation 4 is taken over all the angular springs that involve bond 0-*i* and use particle 0 as the pivots.

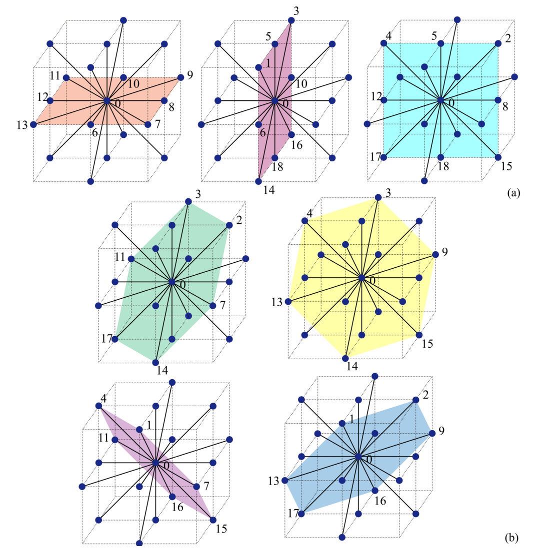

Figure 3. Planes of the body-centered lattice model. (a) *xy-, xz-, yz-* planes with 8 particles on each plane (b) four hexagonal planes with 6 particles on each plane.

Another critical part of this dynamic lattice method is to find its connection with the anisotropic medium. In order to create anisotropy in the lattice model we set the stiffness coefficient according to the corresponding linear springs and angular springs. Comparing the elastic energy density in the lattice unit with the strain energy in the anisotropic continuum, we can get the relation between the stiffness coefficients and the elasticity tensor of the arbitrary anisotropic medium. Since there exists 18 particles around the central particle, in the 7 planes (*xy-, yz-, zx-* and the four hexagonal planes) of one lattice unit, we set several stiffness coefficients for linear springs and angular springs. Considering the symmetry between the stiffness coefficients in the lattice unit, we reduce the independent stiffness coefficients for the linear spring to k_{01}, k_{02}, k_{03}, k_{04}, k_{07}, k_{09} , and the independent stiffness coefficients for the angular springs are given by

$$\begin{aligned}
&b^1_{h1}=b_{2\text{-}0\text{-}3}=b_{17\text{-}0\text{-}14};\ b^2_{h1}=b_{3\text{-}0\text{-}11}=b_{14\text{-}0\text{-}7};\ b^3_{h1}=b_{11\text{-}0\text{-}17}=b_{7\text{-}0\text{-}2};\\
&b^1_{h2}=b_{9\text{-}0\text{-}3}=b_{13\text{-}0\text{-}14};\ b^2_{h2}=b_{3\text{-}0\text{-}4}=b_{14\text{-}0\text{-}15};\ b^3_{h2}=b_{4\text{-}0\text{-}13}=b_{15\text{-}0\text{-}9};\\
&b^1_{h3}=b_{1\text{-}0\text{-}4}=b_{16\text{-}0\text{-}15};\ b^2_{h3}=b_{4\text{-}0\text{-}11}=b_{15\text{-}0\text{-}7};\ b^3_{h3}=b_{11\text{-}0\text{-}16}=b_{7\text{-}0\text{-}1};\\
&b^1_{h4}=b_{2\text{-}0\text{-}1}=b_{17\text{-}0\text{-}16};\ b^2_{h4}=b_{1\text{-}0\text{-}13}=b_{16\text{-}0\text{-}9};\ b^3_{h4}=b_{13\text{-}0\text{-}17}=b_{9\text{-}0\text{-}2};\\
&b_{xy}=b_{6\text{-}0\text{-}7}=b_{7\text{-}0\text{-}8}=b_{8\text{-}0\text{-}9}=b_{9\text{-}0\text{-}10};\\
&b_{xz}=b_{6\text{-}0\text{-}1}=b_{1\text{-}0\text{-}5}=b_{5\text{-}0\text{-}3}=b_{3\text{-}0\text{-}10};\\
&b_{yz}=b_{8\text{-}0\text{-}2}=b_{2\text{-}0\text{-}5}=b_{5\text{-}0\text{-}4}=b_{4\text{-}0\text{-}12};
\end{aligned} \tag{5}$$

where b^1_{h1}, b^2_{h1}, b^3_{h1}, b^1_{h2}, b^2_{h2}, b^3_{h2}, b^1_{h3}, b^2_{h3}, b^3_{h3}, b^1_{h4}, b^2_{h4} and b^3_{h4} are the independent stiffness coefficients for the linear springs in the hexagonal planes while b_{xy}, b_{xz} and b_{yz} are the independent stiffness coefficients for the linear springs in the *xy*-, *xz*- and *yz*-planes. The relative displacement between particles *0* and *i* can be written as

$$\mathbf{u}_i-\mathbf{u}_0=\begin{pmatrix}\dfrac{\partial u_x}{\partial x} & \dfrac{\partial u_x}{\partial y} & \dfrac{\partial u_x}{\partial z}\\ \dfrac{\partial u_y}{\partial x} & \dfrac{\partial u_y}{\partial y} & \dfrac{\partial u_y}{\partial z}\\ \dfrac{\partial u_z}{\partial x} & \dfrac{\partial u_z}{\partial y} & \dfrac{\partial u_z}{\partial z}\end{pmatrix}\begin{pmatrix}R_{0i}^x\\ R_{0i}^y\\ R_{0i}^z\end{pmatrix}\begin{pmatrix}\mathbf{e}_x & \mathbf{e}_y & \mathbf{e}_z\end{pmatrix} \tag{6}$$

where u_x, u_y and u_z respectively denote the *x*-, *y*- and *z*-components of the displacement field while R_{0i}^x, R_{0i}^y and R_{0i}^z represent the *x*-, *y*- and *z*- components of $\boldsymbol{R}_{0i}$ respectively. $\boldsymbol{e}_x$, $\boldsymbol{e}_y$ and $\boldsymbol{e}_z$ are the unit vectors in the *x*-, *y*- and *z*-directions respectively. Meanwhile the strain tensor is given by

$$\begin{aligned}
\varepsilon_{xx}&=\frac{\partial u_x}{\partial x}; \quad \varepsilon_{xy}=\varepsilon_{xy}=\frac{1}{2}\left(\frac{\partial u_x}{\partial y}+\frac{\partial u_y}{\partial x}\right);\\
\varepsilon_{yy}&=\frac{\partial u_y}{\partial y}; \quad \varepsilon_{xz}=\varepsilon_{zx}=\frac{1}{2}\left(\frac{\partial u_x}{\partial z}+\frac{\partial u_z}{\partial x}\right);\\
\varepsilon_{zz}&=\frac{\partial u_z}{\partial z}; \quad \varepsilon_{yz}=\varepsilon_{zy}=\frac{1}{2}\left(\frac{\partial u_z}{\partial y}+\frac{\partial u_y}{\partial z}\right).
\end{aligned} \tag{7}$$

The elastic energy in the 3D lattice unit can be written as

$$\begin{aligned}
E=&S_1\varepsilon_{xx}^2+S_2\varepsilon_{yy}^2+S_3\varepsilon_{zz}^2+S_4\varepsilon_{xy}^2+S_5\varepsilon_{xz}^2+S_6\varepsilon_{yz}^2+S_7\varepsilon_{xx}\varepsilon_{xy}\\
&+S_8\varepsilon_{xx}\varepsilon_{xz}+S_9\varepsilon_{xx}\varepsilon_{yz}+S_{10}\varepsilon_{yy}\varepsilon_{xy}+S_{11}\varepsilon_{yy}\varepsilon_{xz}+S_{12}\varepsilon_{yy}\varepsilon_{yz}\\
&+S_{13}\varepsilon_{zz}\varepsilon_{xy}+S_{14}\varepsilon_{zz}\varepsilon_{xz}+S_{15}\varepsilon_{zz}\varepsilon_{yz}+S_{16}\varepsilon_{xx}\varepsilon_{yy}+S_{17}\varepsilon_{xx}\varepsilon_{zz}\\
&+S_{18}\varepsilon_{yy}\varepsilon_{zz}+S_{19}\varepsilon_{xy}\varepsilon_{xz}+S_{20}\varepsilon_{xy}\varepsilon_{yz}+S_{21}\varepsilon_{xz}\varepsilon_{yz}
\end{aligned} \tag{8}$$

where

$$\begin{aligned}
S_1=&\frac{1}{16}\left(b_{h1}^1+b_{h1}^2+b_{h2}^2+b_{h2}^3+b_{h3}^2+b_{h3}^3+b_{h4}^1+b_{h4}^2\right)\\
&+\frac{1}{4}\left(b_{h1}^3+b_{h2}^1+b_{h3}^1+b_{h4}^3\right)+2\left(b_{xy}+b_{xz}\right)\\
&+\frac{a^2}{4}\left(k_{0\text{-}1}+k_{0\text{-}3}+k_{0\text{-}7}+k_{0\text{-}9}\right);
\end{aligned} \tag{9}$$

$$\begin{aligned}
S_2=&\frac{1}{16}\left(b_{h1}^2+b_{h1}^3+b_{h2}^1+b_{h2}^2+b_{h3}^1+b_{h3}^2+b_{h4}^2+b_{h4}^3\right)\\
&+\frac{1}{4}\left(b_{h1}^1+b_{h2}^3+b_{h3}^3+b_{h4}^1\right)+2\left(b_{xy}+b_{yz}\right)\\
&+\frac{a^2}{4}\left(k_{0\text{-}2}+k_{0\text{-}4}+k_{0\text{-}7}+k_{0\text{-}9}\right);
\end{aligned} \tag{10}$$

$$\begin{aligned}
S_3=&\frac{1}{16}\left(b_{h1}^1+b_{h1}^3+b_{h2}^1+b_{h2}^3+b_{h3}^1+b_{h3}^3+b_{h4}^1+b_{h4}^3\right)\\
&+\frac{1}{4}\left(b_{h1}^2+b_{h2}^2+b_{h3}^2+b_{h4}^2\right)+2\left(b_{xz}+b_{yz}\right)\\
&+\frac{a^2}{4}\left(k_{0\text{-}2}+k_{0\text{-}4}+k_{0\text{-}7}+k_{0\text{-}9}\right);
\end{aligned} \tag{11}$$

$$\begin{aligned}
S_4=&\frac{1}{4}\left(b_{h1}^1+b_{h1}^3+b_{h2}^1+b_{h2}^3+b_{h3}^1+b_{h3}^3+b_{h4}^1+b_{h4}^3\right)\\
&+b_{h1}^2+b_{h2}^2+b_{h3}^2+b_{h4}^2+a^2\left(k_{0\text{-}7}+k_{0\text{-}9}\right);
\end{aligned} \tag{12}$$

$$\begin{aligned}
S_5=&\frac{1}{4}\left(b_{h1}^2+b_{h1}^3+b_{h2}^1+b_{h2}^2+b_{h3}^1+b_{h3}^2+b_{h4}^2+b_{h4}^3\right)\\
&+b_{h1}^1+b_{h2}^3+b_{h3}^3+b_{h4}^1+a^2\left(k_{0\text{-}1}+k_{0\text{-}3}\right);
\end{aligned} \tag{13}$$

$$\begin{aligned}
S_6=&\frac{1}{4}\left(b_{h1}^1+b_{h1}^2+b_{h2}^2+b_{h2}^3+b_{h3}^2+b_{h3}^3+b_{h4}^1+b_{h4}^2\right)\\
&+b_{h1}^3+b_{h2}^1+b_{h3}^1+b_{h4}^3+a^2\left(k_{0\text{-}2}+k_{0\text{-}4}\right);
\end{aligned} \tag{14}$$

$$\begin{aligned}
S_7=&\frac{1}{2}\left(-b_{h1}^2-b_{h1}^3+b_{h2}^1+b_{h2}^2-b_{h3}^1-b_{h3}^2+b_{h4}^2+b_{h4}^3\right)\\
&+\frac{1}{4}\left(b_{h1}^1-b_{h2}^3+b_{h3}^1-b_{h4}^3\right)+a^2\left(k_{0\text{-}7}-k_{0\text{-}9}\right);
\end{aligned} \tag{15}$$

$$\begin{aligned}
S_8=&\frac{1}{2}\left(b_{h1}^1+b_{h1}^3-b_{h2}^1-b_{h2}^3-b_{h3}^1-b_{h3}^3+b_{h4}^1+b_{h4}^3\right)\\
&+\frac{1}{4}\left(-b_{h1}^2+b_{h2}^2+b_{h3}^2-b_{h4}^2\right)+a^2\left(k_{0\text{-}1}-k_{0\text{-}3}\right);
\end{aligned} \tag{16}$$

$$\begin{aligned}
S_9=&\frac{1}{4}\left(-b_{h1}^1-b_{h1}^2-b_{h2}^2-b_{h2}^3+b_{h3}^2+b_{h3}^3+b_{h4}^1+b_{h4}^2\right)\\
&-b_{h1}^3-b_{h2}^1+b_{h3}^1+b_{h4}^3;
\end{aligned} \tag{17}$$

$$\begin{aligned}
S_{10}=&\frac{1}{2}\left(-b_{h1}^1-b_{h1}^2+b_{h2}^2+b_{h2}^3-b_{h3}^2-b_{h3}^3+b_{h4}^1+b_{h4}^2\right)\\
&+\frac{1}{4}\left(b_{h1}^3-b_{h2}^1+b_{h3}^1-b_{h4}^3\right)+a^2\left(k_{0\text{-}7}-k_{0\text{-}9}\right);
\end{aligned} \tag{18}$$

$$\begin{aligned}
S_{11}=&\frac{1}{4}\left(-b_{h1}^2-b_{h1}^3+b_{h2}^1+b_{h2}^2+b_{h3}^1+b_{h3}^2-b_{h4}^2-b_{h4}^3\right)\\
&-b_{h1}^1+b_{h2}^3+b_{h3}^3-b_{h4}^1;
\end{aligned} \tag{19}$$

$$\begin{aligned}
S_{12}=&\frac{1}{2}\left(b_{h1}^1+b_{h1}^3+b_{h2}^1+b_{h2}^3-b_{h3}^1-b_{h3}^3-b_{h4}^1-b_{h4}^3\right)\\
&+\frac{1}{4}\left(-b_{h1}^2-b_{h2}^2+b_{h3}^2+b_{h4}^2\right)+a^2\left(k_{0\text{-}4}-k_{0\text{-}2}\right);
\end{aligned} \tag{20}$$

$$\begin{aligned}
S_{13}=&\frac{1}{4}\left(b_{h1}^1+b_{h1}^3-b_{h2}^1-b_{h2}^3+b_{h3}^1+b_{h3}^3-b_{h4}^1-b_{h4}^3\right)\\
&+b_{h1}^2-b_{h2}^2+b_{h3}^2-b_{h4}^2;
\end{aligned} \tag{21}$$

$$\begin{aligned}
S_{14}=&\frac{1}{2}\left(b_{h1}^1+b_{h1}^2-b_{h2}^2-b_{h2}^3-b_{h3}^2-b_{h3}^3+b_{h4}^1+b_{h4}^2\right)\\
&+\frac{1}{4}\left(-b_{h1}^3+b_{h2}^1+b_{h3}^1-b_{h4}^3\right)+a^2\left(k_{0\text{-}1}-k_{0\text{-}3}\right);
\end{aligned} \tag{22}$$

$$\begin{aligned}
S_{15}=&\frac{1}{2}\left(b_{h1}^2+b_{h1}^3+b_{h2}^1+b_{h2}^2-b_{h3}^1-b_{h3}^2-b_{h4}^2-b_{h4}^3\right)\\
&+\frac{1}{4}\left(-b_{h1}^1-b_{h2}^3+b_{h3}^1+b_{h4}^3\right)+a^2\left(k_{0\text{-}4}-k_{0\text{-}2}\right);
\end{aligned} \tag{23}$$

$$\begin{aligned}
S_{16}=&-\frac{1}{4}\left(b_{h1}^1+b_{h1}^3+b_{h2}^1+b_{h2}^3+b_{h3}^1+b_{h3}^3+b_{h4}^1+b_{h4}^3\right)\\
&+\frac{1}{8}\left(b_{h1}^2+b_{h2}^2+b_{h3}^2+b_{h4}^2\right)+\frac{a^2}{2}\left(k_{0\text{-}7}-k_{0\text{-}9}\right)-4b_{xy};
\end{aligned} \tag{24}$$

$$\begin{aligned}
S_{17}=&-\frac{1}{4}\left(b_{h1}^2+b_{h1}^3+b_{h2}^1+b_{h2}^2+b_{h3}^1+b_{h3}^2+b_{h4}^2+b_{h4}^3\right)\\
&+\frac{1}{8}\left(b_{h1}^1+b_{h2}^3+b_{h3}^3+b_{h4}^1\right)+\frac{a^2}{2}\left(k_{0\text{-}1}-k_{0\text{-}3}\right)-4b_{xz};
\end{aligned} \tag{25}$$

$$\begin{aligned}
S_{18}=&-\frac{1}{4}\left(b_{h1}^1+b_{h1}^2+b_{h2}^2+b_{h2}^3+b_{h3}^2+b_{h3}^3+b_{h4}^1+b_{h4}^2\right)\\
&+\frac{1}{8}\left(b_{h1}^3+b_{h2}^1+b_{h3}^1+b_{h4}^3\right)+\frac{a^2}{2}\left(k_{0\text{-}2}-k_{0\text{-}4}\right)-4b_{yz};
\end{aligned} \tag{26}$$

$$\begin{aligned}
S_{19}=&b_{h1}^1+b_{h1}^2+b_{h2}^2+b_{h2}^3-b_{h3}^2-b_{h3}^3-b_{h4}^1-b_{h4}^2\\
&+\frac{1}{2}\left(-b_{h1}^3-b_{h2}^1+b_{h3}^1+b_{h4}^3\right);
\end{aligned} \tag{27}$$

$$S_{20} = b_{h1}^2 + b_{h1}^3 - b_{h2}^1 - b_{h2}^2 + b_{h3}^1 + b_{h3}^2 - b_{h4}^2 - b_{h4}^3 + \frac{1}{2}\left(-b_{h1}^1 + b_{h2}^3 - b_{h3}^1 + b_{h4}^3\right); \tag{28}$$

$$S_{21} = -b_{h1}^1 - b_{h1}^3 + b_{h2}^1 + b_{h2}^3 - b_{h3}^1 - b_{h3}^3 + b_{h4}^1 + b_{h4}^3 + \frac{1}{2}\left(b_{h1}^2 - b_{h2}^2 + b_{h3}^2 - b_{h4}^2\right); \tag{29}$$

and here $a = |\boldsymbol{R}_{0i}|$. On the other hand, the elastic energy density, φ, for the arbitrary anisotropic media is given by

$$\begin{aligned}\varphi = {} & \frac{1}{2}C_{11}\varepsilon_{xx}^2 + \frac{1}{2}C_{22}\varepsilon_{yy}^2 + \frac{1}{2}C_{33}\varepsilon_{zz}^2 + 2C_{44}\varepsilon_{xy}^2 + 2C_{55}\varepsilon_{xz}^2 + 2C_{66}\varepsilon_{yz}^2 \\ & + 2C_{14}\varepsilon_{xx}\varepsilon_{xy} + 2C_{15}\varepsilon_{xx}\varepsilon_{xz} + 2C_{16}\varepsilon_{xx}\varepsilon_{yz} + 2C_{24}\varepsilon_{yy}\varepsilon_{xy} + 2C_{25}\varepsilon_{yy}\varepsilon_{xz} \\ & + 2C_{26}\varepsilon_{yy}\varepsilon_{yz} + 2C_{34}\varepsilon_{zz}\varepsilon_{xy} + 2C_{35}\varepsilon_{zz}\varepsilon_{xz} + 2C_{36}\varepsilon_{zz}\varepsilon_{yz} + C_{12}\varepsilon_{xx}\varepsilon_{yy} \\ & + C_{13}\varepsilon_{xx}\varepsilon_{zz} + C_{23}\varepsilon_{yy}\varepsilon_{zz} + 4C_{46}\varepsilon_{xy}\varepsilon_{yz} + 4C_{45}\varepsilon_{xy}\varepsilon_{xz} + 4C_{56}\varepsilon_{xz}\varepsilon_{yz}\end{aligned} \tag{30}$$

where C_{ij} represent the independent components of the elasticity tensor of the anisotropic medium. In order to simulate the anisotropic media, we let the elastic energy stored in the lattice unit equal the elastic energy stored in the effective volume of the anisotropic media. Therefore, the connection between the stiffness coefficients and the elasticity tensor lies in

$$E = V_{eff}\varphi \tag{31}$$

The effective volume of this body-centered elastic model held by each lattice unit is $V_{eff} = 2a^3$. combining the equations from 8 to 31, we can get the linear transformation between the independent stiffness coefficients and the elasticity tensor of the anisotropic medium. According to equation 3, we can get the interaction force on the central particle *0* with the linear transformation of the independent stiffness coefficients. And here we use GPU(GeForce RTX 3090) to accelerate the calculation of force by transforming the calculated stiffness coefficients from CPU device to GPU device and then do the computing of the forces on GPU device. Once the forces of the particles are given, the displacement of the particles are calculated by the Verlet accumulation which is written as

$$\mathbf{u}_i(t_0 + \Delta t) = 2\mathbf{u}_i(t_0) - \mathbf{u}_i(t_0 - \Delta t) + \frac{\mathbf{f}_i(t_0)}{m_i}\Delta t^2 \tag{32}$$

where Δt is the time stepping, $\boldsymbol{f}_i$ is the total force on particle i and m_i represents the mass of particle i. Therefore, with the initial dynamics of particle along with the boundary we can calculate the dynamics of the particles at each time step.

Numerical examples

A complex lattice model is used to simulate the elastic wave propagation in anisotropic media. The elastic properties of the anisotropic medium are chosen according to the standard model given by Igel et al. (1995) and we use the velocity and density of the SEG overthrust model to replace the C_{ij} of the following elasticity tensor with the following equation

$$e_{ijknm} = v_{ijk} * v_{ijk} * \rho_{ijk} * C_{nm} / C_{33} \tag{33}$$

$$C_{nm} = \begin{pmatrix} 10.0 & 3.5 & 2.5 & -5.0 & 0.1 & 0.3 \\ 3.5 & 8.0 & 1.5 & 0.2 & -0.1 & -0.15 \\ 2.5 & 1.5 & 6.0 & 1.0 & 0.4 & 0.24 \\ -5.0 & 0.2 & 1.0 & 5.0 & 0.35 & 0.525 \\ 0.1 & -0.1 & 0.4 & 0.35 & 4.0 & -1.0 \\ 0.3 & -0.15 & 0.24 & 0.525 & -1.0 & 3.0 \end{pmatrix} \tag{34}$$

We use the Ricker wavelet with 20 Hz dominant frequency as the source time function. The lattice spacing for this numerical test is 5 m and the time stepping is 0.2ms. We place a single force at the center of the test area.

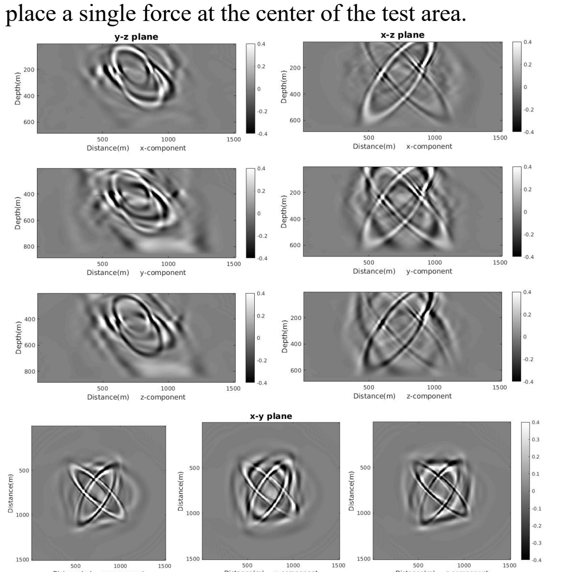

Figure 4: The snapshots simulated by DLM in the anisotropic medium at 0.16s of *x*-,*y*- and *z*-component in the three planes.

Conclusion

We development a body-centered 3D anisotropic lattice model to simulate the dynamic behavior. The connection between the stiffness coefficients of the lattice model and the elasticity tensor is derived. Therefore, we can translate the elastic properties of the anisotropic media into particle interaction. This development allows numerical simulation of various kinds of behaviors the anisotropic media. Our numerical experiments show that DLM is capable of simulating elastic waves in arbitrary anisotropic media.

Acknowledgments

The authors acknowledge critical comments from Dr. Xiaolin Hu and also thank Yuhang Wang for his fruitful discussions. This study received support from National Natural Science Foundation of China (No. 42074125).